Application of Scanning Nonlinear Dielectric Microscopy to Measurement of Dopant Profiles in Transistors

● Koichiro Honda

(Manuscript received December 28, 2009)

This paper presents results obtained when using scanning nonlinear dielectric microscopy (SNDM) to measure dopant profiles in transistors. Secondary ion mass spectrometry (SIMS) measurements of an epitaxial multilayer film on a standard sample and SNDM measurements of the sample surface showed that it was possible to obtain a uniform concentration region with a thickness of approximately 4–5 μm in each layer. An SNDM signal with a one-to-one correspondence to the dopant quantity was obtained. In real devices, dopant concentration profiles could be obtained as two-dimensional images by applying calibration curves from the standard sample to cross-sectional observations of n- and p-channel transistors.

1. Introduction

In the source/drain analysis of semiconductor transistors, accurate measurements of the two-dimensional concentration profiles of carriers and dopants implanted to form these transistors are crucial for the design and analysis of LSIs. A number of methods have been advocated for this purpose.[1] One practical application is electron holography using a transmission electron microscope (TEM).[2] Another is scanning probe microscopy (SPM), which includes scanning capacitance microscopy (SCM)[3] and scanning spreading resistance microscopy (SSRM).[4] Although each technique has its own strong points, SPM-based methods are thought to be advantageous due to the ease of sample preparation. They use an atomic force microscope (AFM) equipped with a conductive cantilever that can be scanned across the sample to measure the capacitance distribution with respect to an externally applied voltage (in SCM) or the resistance distribution (in SSRM), for example. Developments are being made in each of these techniques.

In a previous study, my coworkers and I clarified the effectiveness of scanning nonlinear dielectric microscopy (SNDM), which is one SPM implementation. It has mainly been used to observe the distribution of polarization in ferroelectric materials.[5)–9)] For thin ferroelectric films, the polarization direction can be determined from the nonlinear permittivity obtained from the SNDM signal. Previous papers have reported on the use of this method in applications such as observing the polarization distribution of $LiTaO_3$ and the thickness of polarization domain walls in $PbZr_xTi_{1-x}$ (lead zirconate titanate) and retrieving data recorded in ferroelectric memory using nanodomains. Success in the visualization of charges in nonvolatile flash memories has been achieved by applying SNDM to semiconductor measurements.[10),11)] SNDM has been reported to be capable of detecting the 7×7 structure of a clean Si surface by performing high-resolution observations under high vacuum conditions.[12)] Therefore, SNDM is promising as

another microscopy method for dopant profile measurement.

In this paper, I report on the measurement of dopant concentration profiles in transistors with the aim of applying SNDM to LSI device analysis.

2. SNDM principles and measurement methods

2.1 Basic principles

SNDM is a microwave microscopy technique. To measure the charge distribution over a very small region, we use an AFM with a ring electrode attached to the conductive cantilever. The general configuration of an SNDM system is shown in **Figure 1**.[5)–8)]

When an alternating electric field $E\cos\omega_p t$ ($E = V/d$, where V is the voltage amplitude and d is the sample thickness, ω_p = angular frequency) is applied between an electrode (probe tip) and the test piece, the change in capacitance $C_s(t)$ that arises from the nonlinear dielectric response of the sample surface beneath the probe is detected as a change in the resonant frequency of an LC resonator circuit. This capacitance change $\Delta C_s(t)$ is given by

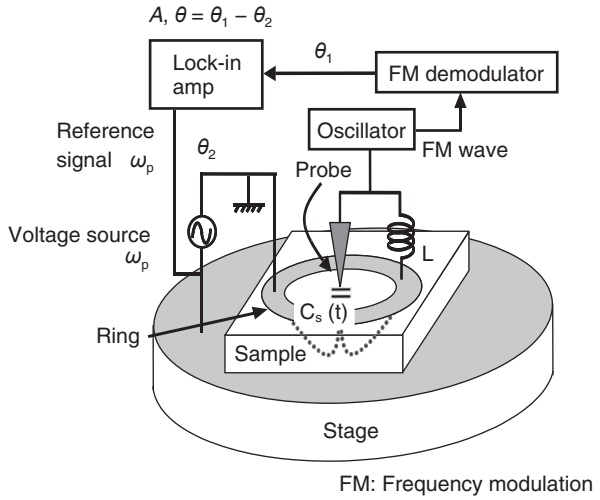

Figure 1
Outline of SNDM system.

$$\Delta C_s(t)/C_{s0} = (\varepsilon_{333}/\varepsilon_{33})E\cos\omega_p t + (\varepsilon_{3333}/\varepsilon_{33})/4 \cdot E^2\cos 2\omega_p t + \ldots, \quad (1)$$

whence

$$dC_s(t)/dV \approx \varepsilon_{333}/\varepsilon_{33},\ d^2C_s(t)/dV^2 \approx \varepsilon_{3333}/\varepsilon_{33}. \quad (2)$$

Here, ε_{33} is the linear permittivity, ε_{333} is the lowest-order nonlinear permittivity, ε_{3333} is the second-order nonlinear permittivity, and C_{s0} is the electrostatic capacitance, which is proportional to ε_{33}. From this formula, ε_{333} can be obtained by detecting the ω_p component of the SNDM signal, and higher-order nonlinear permittivity parameters ε_{3333} and above can be obtained by detecting the higher-order components of $2\omega_p$ and above. The capacitance change produced by the nonlinear dielectric response is very small [$\Delta C_s(t)/C_{s0} = 10^{-3} – 10^{-8}$], and the SNDM sensitivity is roughly 10^{-22} F. This value is considerably better than the SCM's sensitivity, which is usually around 10^{-18} F. Incidentally, the higher-order nonlinear permittivity components are the coefficients of the higher-order powers of the electric field E. The higher-order powers of E are concentrated in a localized space, so the higher-order nonlinear components are only obtained from localized regions. Since SNDM's superior sensitivity lets it detect the higher-order permittivity terms in Equation (1) with a high signal-to-noise ratio, it can achieve higher spatial resolution by detecting the higher-order components of $2\omega_p$ and above.[9)]

From Equation (1), by determining the ω_p component in SNDM, we can obtain the nonlinear permittivity in the vicinity of the sample surface. When the sample surface has a metal oxide semiconductor (MOS) type structure, this is equivalent to measuring the change in capacitance directly below the MOS interface [Equation (2)], and it is possible to ascertain the change in the depletion layer caused by the dopant concentration in the same way as in SCM. Conversely, it is possible to ascertain the dopant concentration from this change.[13),14)]

2.2 Dopant concentration profile measurement methods

As initial steps towards using SNDM to measure dopant concentration profiles, we fabricated standard samples with known dopant concentrations and measured them using secondary ion mass spectrometry (SIMS) and SNDM to investigate the correlation between the SNDM signal and dopant concentration. The standard samples were epitaxial crystals comprising multiple layers of Si with various dopant concentrations deposited on n-type and p-type substrates. Cross sections through these multilayer epitaxial films were ground to a smooth surface and used as SNDM test samples.

3. Measurement results

3.1 SNDM measurements of standard sample cross sections

Concentration profiles of the epitaxial multilayer films in the standard samples and an example of SNDM measurement results obtained at the cross section are shown in **Figure 2**. Figures 2 (a) and (b) show the concentration profiles obtained by SIMS measurements of samples doped with n-type (P) and p-type (B) impurities, and (c) and (d) show the SNDM images and SNDM signal strength distributions obtained by averaging these images across 32 scan lines. In (c) and (d), layers with a high concentration of n-type dopant appear black while those with a high concentration of p-type dopant appear bright. These results agree with the actual numbers of layers in the samples—five

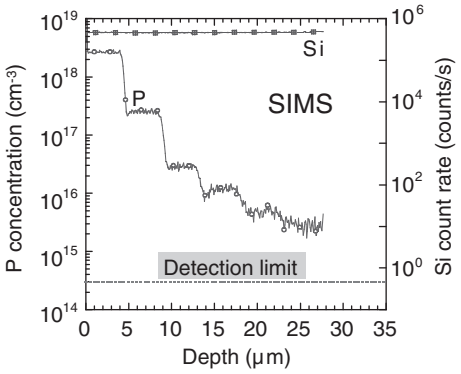

(a) Dopant concentration profile obtained by SIMS measurement of n-type sample (doped with P)

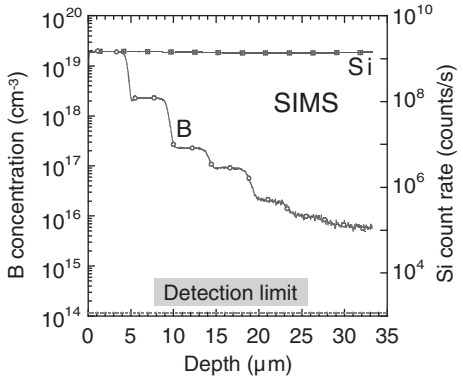

(b) Dopant concentration profile obtained by SIMS measurement of p-type sample (doped with B)

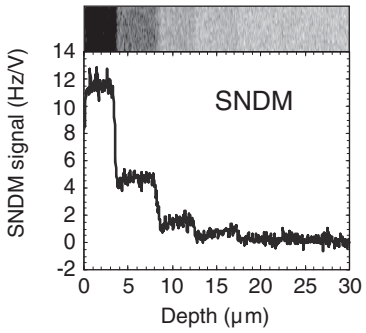

(c) SNDM image and SNDM signal of n-type sample

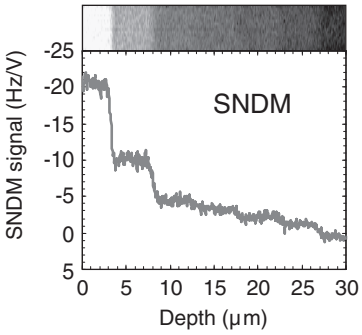

(d) SNDM image and SNDM signal of p-type sample

Figure 2
Results of SIMS and SNDM measurements of standard samples.

layers in the n-type sample and seven layers in the p-type sample—and show that the regions of fixed concentration consisted of steps approximately 4–5 μm thick in the same way as in the SIMS results of (a) and (b).

3.2 Calibration curves for standard samples

SIMS measurement results for the standard samples together with SNDM measurements of the wafer cross sections are shown in **Figure 3.** Figure 3 (a) shows the calibration curves for the SNDM signals and concentration profiles obtained from SIMS data. They were produced by using the depth information in Figure 2 as a common parameter. Figure 3 (b) shows the calibration results for each concentration profile; here, we see a match over concentrations ranging from 1×10^{16} to 1×10^{18} cm^{-3} for n-type doping and from 1×10^{17} to 1×10^{19} cm^{-3} for p-type doping. Since these calibration curves for high concentrations can be approximated by exponential functions, they can be expressed as single-valued functions. Therefore, Figure 3 (a) shows that the SNDM signal can be transformed into a dopant concentration.

In this way, by comparing the SIMS and SNDM measurements of epitaxial multilayer films, we obtained a thickness of approximately 4–5 μm for the constant concentration region in each layer, and we succeeded in obtaining an SNDM signal with a one-to-one correspondence to the dopant concentration.

In earlier dopant profile measurements using SCM, contrast reversal sometimes occurred with a peak value of the order of 10^{18} cm^{-3} for both n- and p-type materials when unbiased. It has been reported that the correlation between the SCM signal and dopant quantity is no longer single-valued unless a DC bias voltage is applied.[15] However, with SNDM, the relationship with the dopant concentration can be expressed as a single-valued function for some sample fabrication methods. This shows that it is possible to compile a database for calibration between SNDM and SIMS.

3.3 Observation of transistor cross sections

We performed SNDM observations of n- and p-channel transistor cross sections as examples of dopant profiles in real devices. By using the calibration curves obtained from the standard samples, we successfully obtained the concentration profiles in two-dimensional images of the transistor cross sections.

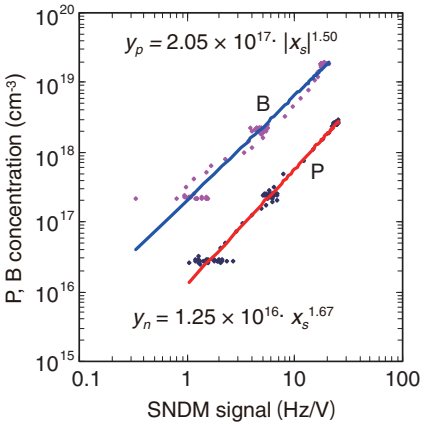

(a) Calibration curve for SNDM signal vs. dopant concentration

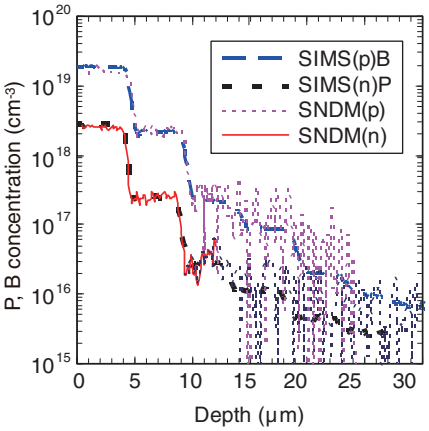

(b) SNDM vs. SIMS calibration results

Figure 3
Calibration curves for standard samples.

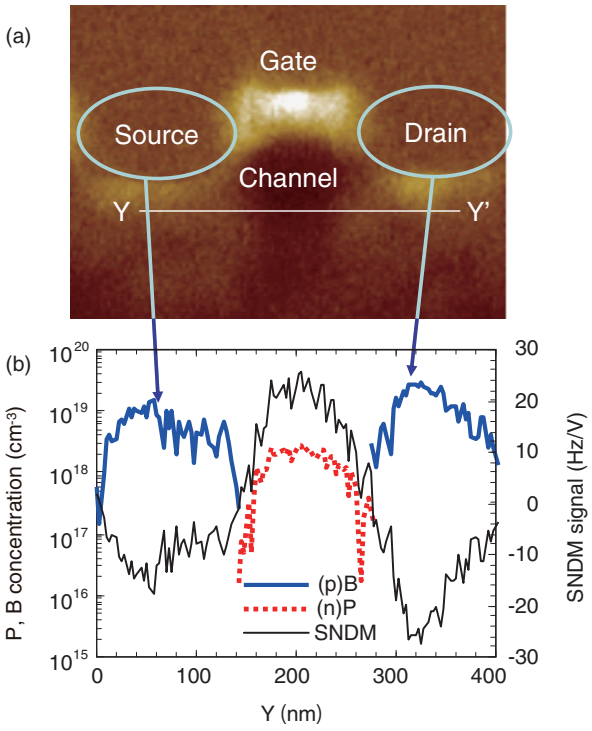

Figure 4
Results of SNDM measurements of p-MOSFET cross section sample. (a) SNDM image and (b) variation in signal strength along line Y–Y'.

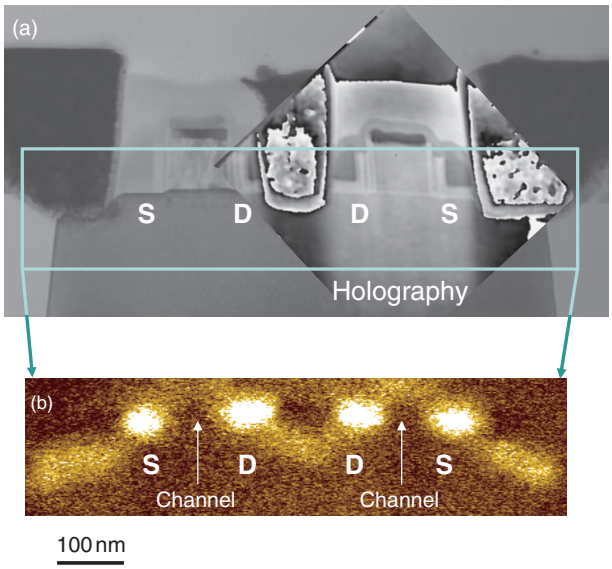

Figure 5
Cross-sectional images of SRAM cell transistors. (a) TEM image and electron beam holography image and (b) SNDM image of the same location.

SNDM measurement results for the cross section of a p-channel transistor are shown in **Figure 4**. Figure 4 (a) is an SDNM image of the transistor cross section sample and Figure 4 (b) shows the signal strength distribution and dopant concentration profile along the line Y–Y' between the source and drain regions. These transistor samples were fabricated under the same processing conditions as the standard samples. By using a calibration curve of the type shown in Figure 3 (a), we were able to convert the SNDM signal into a concentration profile and obtain a two-dimensional concentration profile of the transistor cross section.

The above results indicate that this method can be used to make quantitative measurements of dopant concentration profiles in semiconductor devices. In the future, it will be necessary to investigate whether or not the dopant concentration profiles obtained by these SNDM measurements are valid by comparing them with the results for other techniques such as SSRM. Furthermore, by establishing a reliable quantitative measurement technique, we will apply the technique to process simulators where a two-dimensional concentration profile can be obtained by inputting the process conditions such as the dopant implantation conditions.

3.4 Observation of real device

As an example of application to a real device, we describe the measurement results of a 90-nm static random access memory (SRAM). A cross-sectional TEM image of the p-channel in an SRAM cell transistor together with an SNDM image of the same location are shown in **Figure 5**. An electron holography image is also superimposed on the TEM image. The transistor's channel is very narrow (about 50 nm). The holography image does not provide a dopant phase image because an adequate phase shift could not be obtained. On the other hand, the SNDM image clearly shows a pair of transistor source and drain regions separated by channels.

Thus, SNDM can provide dopant concentration profile images not only from short channels but also from narrow channels.

4. Conclusion

By applying SNDM to the measurement of dopant concentration profiles, we obtained the following results.

1) In SIMS measurements of epitaxial multilayer films and SNDM measurements of wafer cross sections, we obtained a constant-concentration region with a thickness of approximately 4–5 μm in each layer and SNDM signals with a one-to-one correspondence to the dopant quantities.
2) Using a real device, we observed the cross sections of n- and p-channel transistors and obtained the dopant concentration profiles in two-dimensional images of the transistor cross sections by using calibration curves obtained from standard samples.
3) We fabricated test samples of cross sections through miniature devices and obtained SNDM signals from these structures.

We have demonstrated the prospect of expanding SNDM measurement applications from the measurement of dopant concentration profiles in semiconductor devices to defect analysis. In the future, we will apply this technique to the analysis of defects in real devices.

References

1) N. Duhayon et al.: Assessing the performance of two-dimensional dopant profiling techniques. *J. Vac. Sci. Technol.*, Vol. 22, Issue 1, p. 385 (2004).
2) E. Volkl et al.: Introduction to Electron Holography. Edited by E. Volkl, D. Joy, and L. A. Allard, Plenum, New York, 1999.
3) V. V. Zavyalov et al.: Scanning capacitance microscope methodology for quantitative analysis of p-n junctions. *J. Appl. Phys.*, Vol. 85, Issue 11, pp. 7774–7783 (1999).
4) P. De Wolf et al.: Low weight spreading resistance profiling of ultrashallow dopant profiles. *J. Vac. Sci. Technol.*, Vol. 16, Issue 1, pp. 401–405 (1998).
5) Y. Cho et al.: New Microscope for Measuring the Distribution of Nonlinear Dielectric Properties. (in Japanese), *Trans. IEICE*, Vol. J78-C-I, pp. 593–598 (1995).
6) Y. Cho et al.: Scanning Nonlinear Dielectric Microscopy with Nanometer Resolution. *Appl. Phys. Lett.*, Vol. 75, Issue 18, pp. 2833–2855 (1999).
7) H. Odagawa et al.: Theoretical and Experimental Study on Nanoscale Ferroelectric Domain Measurement Using Scanning Nonlinear Dielectric Microscopy. *Jpn. J. Appl. Phys. Part 1*, Vol. 39, No. 9B, pp. 5719–5722 (2000).
8) Y. Cho et al.: Tbit/inch^2 Ferroelectric Data Storage Based on Scanning Nonlinear Dielectric Microscopy. *Appl. Phys. Lett.*, Vol. 81, Issue 23, pp. 4401–4403 (2002).
9) Y. Cho et al.: Measurement of the Ferroelectric Domain Distributions Using Nonlinear Dielectric Response and Piezoelectric Response. *Jpn. J. Appl. Phys.*, Vol. 40, No. 5B, pp. 3544–3548 (2001).
10) K. Honda et al.: Visualization using scanning nonlinear dielectric microscopy of electrons and holes localized in the thin gate film of a metal-SiO_2-Si_3N_4-SiO_2-semiconductor flash memory. *Appl. Phys. Lett.*, Vol. 86, Issue 1, pp. 01351-1–013501-3 (2005).
11) K. Honda et al.: Visualization of charges stored in the floating gate of flash memory by scanning nonlinear dielectric microscopy. *Nanotechnology*, Vol. 17, pp. S185–S188 (2006).
12) R. Hirose et al.: Observation of the Si (111) 7×7 atomic structure using non-contact scanning nonlinear dielectric microscopy. *Nanotechnology*, Vol. 18, 084014 (5pp), (2007).
13) K. Ishikawa et al.: Resolution enhancement in contact-type scanning nonlinear dielectric microscopy using a conductive carbon nanotube probe tip. *Nanotechnology*, Vol. 18 084015 (6pp), (2007).
14) K. Ishikawa et al.: Quantitative Measurement of Dopant Concentration Profiling by Scanning Nonlinear Dielectric Microscopy. MRS 2007 fall meeting, Extended Abstract B12.5.
15) R. Stephenson et al.: Contrast reversal in scanning capacitance microscopy imaging. *Appl. Phys. Lett.*, Vol. 73, Issue 18, pp. 2597–2599 (1998).

Koichiro Honda
Fujitsu Laboratories Ltd.

Dr. Honda received a D.Eng. degree from Tokyo Institute of Technology in 1995. He joined Fujitsu Laboratories Ltd., Kawasaki, Japan in 1977 and engaged in research and development of Si crystals, ferroelectric materials for ICs, and memory devices. He has also been developing methods for determining the characteristics of materials and devices using transmission electron microscopy and scanning probe microscopy. He is a part-time lecturer at the Technology School of Hosei University and a guest professor at the Research Institute of Electrical Communication, Tohoku University. He is a member of the Materials Research Society.